Nano Energy 58 (2019) 536–542

Contents lists available at ScienceDirect

Nano Energy

journal homepage: www.elsevier.com/locate/nanoen

Full paper

A calibration-free self-powered sensor for vital sign monitoring and finger tap communication based on wearable triboelectric nanogenerator

Hui-Jing Qiu[a,1], Wei-Zhi Song[a,1], Xiao-Xiong Wang[a,*], Jun Zhang[a], Zhiyong Fan[b], Miao Yu[a,c], Seeram Ramakrishna[a,d], Yun-Ze Long[a,*]

[a] Collaborative Innovation Center for Nanomaterials & Devices, College of Physics, Qingdao University, Qingdao 266071, China
[b] Department of Electronic & Computer Engineering, The Hong Kong University of Science & Technology, Kowloon, Hong Kong, China
[c] Department of Mechanical Engineering, Columbia University, New York, NY 10027, USA
[d] Center for Nanofibers & Nanotechnology, National University of Singapore, Singapore, Singapore

ARTICLE INFO

Keywords:
Calibration free
Wearable
Triboelectric nanogenerator
Electrospinning
Energy harvesting

ABSTRACT

Triboelectric nanogenerators (TENGs) have attracted much attention due to the high output, low cost, and environmentally friendly nature. However, wearable devices still have certain hardness due to the choice of metal electrode, which has no gas permeability, and affects the wearing comfort. In addition, the electrode does not adhere firmly to the friction material, which also affects the electric performance. We report a TENG base on ordinary fabrics with polymerizes polyaniline (PANI) as electrodes, and uses polycaprolactone (PCL) to make the fabric and friction material fit well. The TENG have excellent softness and certain gas permeability, improving the comfort of the wearable smart health monitoring. The output electrical of TENG can arrive 200 μA and 1000 V under a frequency of 2.5 Hz. It can drive about 1000 LEDs and continuously supply power to electronic production. This truly wearable generator can provide a good information interface for critically ill patients. On the one hand, it can monitor the patient's breathing state in real time and give an alarm when the breathing stops. On the other hand, patients with language communication difficulty can also tap the finger to send messages by using Morse code. More importantly, we have experimentally proved that this self-powered sensor can still work normally with additional contact resistance, which will guarantee the long-term reliable operation of this device in a flexible environment.

1. Introduction

At present, one important direction of electronic products is pursuing for the combination of flexibility, miniaturization and portability, while bringing great demand for mobile energy. Nanogenerators (NGs) can convert mechanical energy into electrical energy in the nanoscale range, being small, lightweight and environmental friendly, to meet the developing needs of electronic product [1,2]. NGs exist in the forms of piezoelectric [3–8], pyroelectric [9–13] and triboelectric [14–17], which can convert various forms of energy in human living environment into electrical energy. Especially, the triboelectric nanogenerators (TENGs) have advantages in NGs due to the high voltage, high efficiency at low frequency, cost efficiency, multiple working modes and material choices [18–20].

Since the concept of TENGs was first proposed in 2012 [21], materials and structures have been continuously optimized to improve the power density for popularization in the portable wearable field [22–27]. However, common electrode materials are metals like aluminum, copper or gold [28,29], leading to a certain hardness of the triboelectric NGs, which will seriously affect the flexibility of the device [30–36]. Compared with the stretchable polymer friction layer, the stress distribution on the metal foil layer is more concentrated, leading to poor anti-sweat corrosion ability. Meanwhile, metal materials are commonly less stable under the sweat erosion. These limited application of NGs with metal electrodes on fabrics. In fact, due to the self-powered nature and excellent anti-static damage performance, NGs have their own irreplaceable stability advantages in the wearable field. Therefore, it is necessary to develop wearable self-powered sensors that can work stably.

In this work, we designed a TENG based on ordinary fabrics with polymerizes polyaniline (PANI) as electrodes. Polycaprolactone (PCL) with low melting point was used to make the fabric and friction

* Corresponding authors.
E-mail addresses: wangxiaoxiong@qdu.edu.cn (X.-X. Wang), yunze.long@qdu.edu.cn (Y.-Z. Long).
[1] These two authors contributed equally to this work.

https://doi.org/10.1016/j.nanoen.2019.01.069
Received 3 January 2019; Received in revised form 21 January 2019; Accepted 27 January 2019
Available online 31 January 2019

material fit well. The generator exhibits excellent softness, and it can perform any folding, kneading, twist operation and so on like ordinary clothes without any influence on the performance of the NG. The TENG can illuminate LEDs or power small electronic devices. A respiratory monitor and a real-time communication based on the TENG can also be designed. It has a great convenience especially for patients with language barriers, and has great application potential in the wearable field. More importantly, we have experimentally proved that this self-powered sensor can still work normally with additional contact resistance, which will guarantee the long-term reliable operation of this device in a flexible environment.

2. Experimental section

2.1. Materials

Polyvinylidene fluoride (PVDF) powders (Mw~600,000), thermoplastic polyurethane (TPU, K985A, Jiangsu Kesu Import & Export Co., Ltd.), polycaprolactone (PCL, average molecular weight of 80,000, SOLVAY) were used in this work. Nylon 6 (PA6) powders was supplied by Macklin Biochemical Co., Ltd., China. N, N-dimethylformamide (DMF), tetrahydrofuran (THF), formic acid, acetic acid and ethanol were obtained from Sinopharm Chemical Reagent Co., Ltd., China. Acetone was obtained from Laiyang Fine Chemical Factory, China. Polyaniline (PANI) synthesized from aniline (Mw = 93.13, Tianjin Bodi Chemical Co., Ltd.), sulfosalicylic acid (SSA, Mw = 254.22, Sinopharm Chemical Reagent Co., Ltd.) and ammonium persulfate (APS, Mw = 228.20, Sinopharm Chemical Reagent Co., Ltd.).

2.2. Preparation of solutions for electrospinning

PVDF homogeneous solution with a consistence of 20 wt% was prepared that the PVDF powder dissolve in an acetone-DMF solvent mixture (1/1 w/w) and then stirred for 4 h at 45 °C. For preparation of the PA6 solution, the polymer was dissolved in formic acid-acetic acid (1/1 w/w) and was continuously stirred for 4 h at room temperature to obtain the transparent solution with a concentration of 15 wt%. The TPU powder was dissolved in DMF-THF solvent mixture (1/1 w/w) and stirred for 3 h at 35 °C to became a homogeneous solution with a concentration of 14 wt%. PCL powder was dissolved in acetone at 30 °C for 3 h to prepare the PCL solution (16 wt%).

2.3. Fabrication of the NG

The schematic of the electrospinning process is shown in the Fig. S1. After in-situ polymerization of PANI as a conductive substrate in conventional cloth, fix the conductive cloth on a drum, covering PCL, TPU and PVDF in proper sequence by electrospinning to prepare the TENG negative material. PCL nanofibers membrane was fabricated under temperature of 27 ± 3 °C and humidity of 55 ± 5%. The polymer solution was supported with a constant flow rate of 0.5 mL h^{-1}, applying a high voltage of 12 kV, and a drum collector was placed 15 cm away from the needle to collect the nanofibers. TPU nanofibers membrane were fabricated under temperature of 25 ± 3 °C and humidity of 42 ± 5%, the feed rate was set 1 mL h^{-1}, electrospinning voltage was 13 kV, and a distance between spinneret and collector was 15 cm. Finally, a layer of PVDF was deposited on the three layered backbone of the negative membrane. PVDF nanofibers membrane was produced under the temperature of 25 ± 3 °C and the humidity of 42 ± 5%, the feed rate was 1 mL h^{-1}, electrospinning voltage was 15 kV, and the distance between spinneret and collector was 15 cm.

The positive material of TENG was prepared similarly. Conductive cloth was chosen as substrate, followed by electrospinning PCL, TPU and PA6 in proper order. PA6 nanofibers membrane was fabricated under temperature of 24 ± 3 °C and humidity of 47 ± 5%, flow rate was 0.5 mL h^{-1}, applying a high voltage of 16 kV, and a drum collector was placed 15 cm away from the needle to collect the nanofibers.

2.4. Characterization and measurements

The surface morphological and microstructures of the TENG were performed on a scanning electron microscope (SEM, TM-1000, Hitachi). The output current signals of the TENG were acquired using a picoammeter (Keithley 6487), the output voltages were recorded using a digital oscilloscope (DSO-X 3024 A, Agilent and GDS-2102, Gwinstek) and the charging voltages of the capacitor were performed with a digital multimeter (Rigol DM 3058). The gas permeability was tested by the gas transmission rate tester (TEXTEST FX 3300). The tensile behavior of the TENG was measured by an Instron 3300 Universal Testing Systems. Fiber membrane adhesion were performed by a digital force

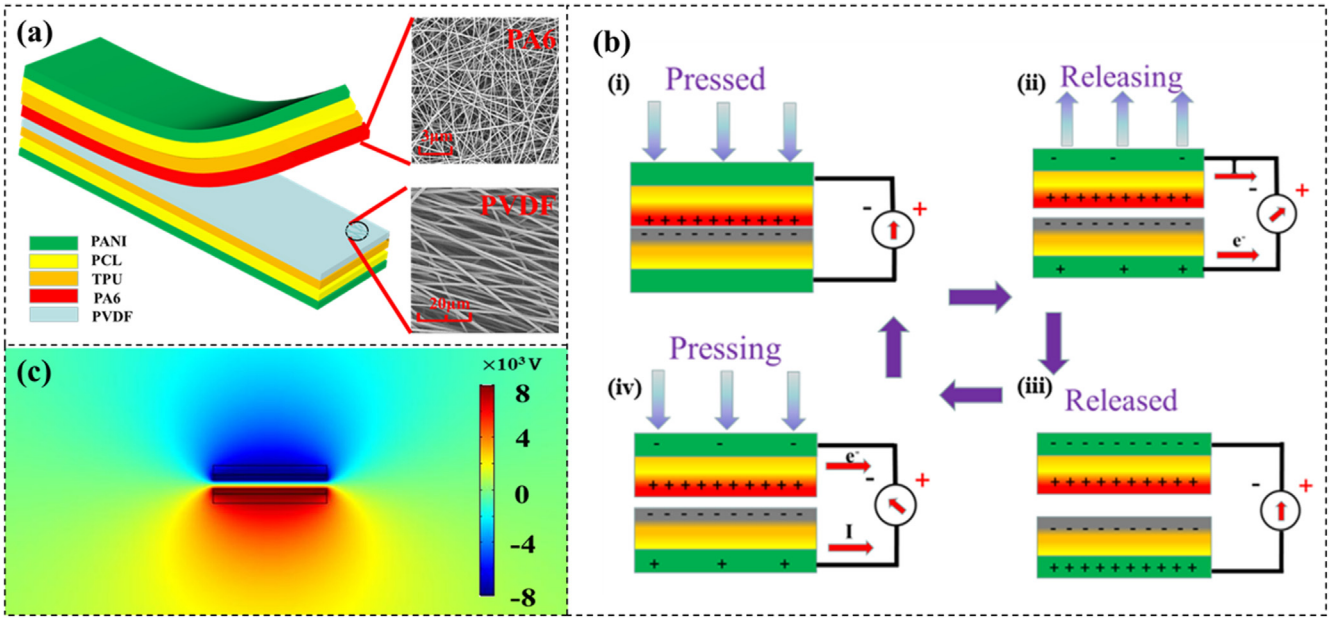

Fig. 1. (a) Structural design of the wearable TENG and SEM image of PA6 and PVDF nanofibers membrane. (b) Electricity generation mechanism of the contact-separation TENG. (c) Simulation of the potential distribution between two triboelectric materials using COMSOL.

gauge (AIGU 2P-5). Ultra-high speed information acquisition card (USB_HRF4826) was used to collect output signals of finger tapping. To generate triboelectric power by the NG, we used a home-made apparatus which could exert periodic contact; the schematic and working principle of this apparatus are shown in Fig. S2.

3. Results and discussion

3.1. The basic characterization of the TENG

As schematically shown in Fig. 1a, the electrospinning nanofibers membrane constituted wearable TENG has multiple layers, PA6 and PVDF act as friction materials. Average diameters of PA6 and PVDF nanofibers were determined to be 120 nm and 970 nm, respectively by SEM image. SEM image of hot pressed crosslinked layer and TPU are present in Fig. S3c and S3d.

The traditional cloth polymerized by PANI in situ works as a conductive substrate supporting the following layers [37–39]. SEM images of fabric fiber and fiber polymerized by PANI are shown in Fig. S3a and S3b. Typically, a simple TENG consists of two electrodes and two triboelectric layers. Fig. 1b shows the working principle of the TENG. Considering the electron affinity difference, PA6 nanofibers were chosen as the positive triboelectric layers, PVDF nanofibers were chosen as the negative triboelectric layers. At the initial state (i), PVDF film and PA6 film were in contact and there was no current flow or electrical potentials. Due to different surface electron affinities, the charges will be transferred from the PA6 film surface to the PVDF film surface, leaving net positive charges on the PA6 nanofibers surface and net negative charges on the PVDF nanofibers surface. When separated, the resulting charge separation will induce a potential difference across the conductive cloth causing subsequent current flow if the device is connected to an external circuit (state ii). At the maximum separation distance, the positive open-circuit was decreased to zero (state iii). The current flow was reversed when the two charged surfaces were brought into contact again (state iv) [34,40–42]. Without any touch, no charge was transferred. Fig. 1c show the simulation of the potential distribution between two triboelectric materials by COMSOL.

As shown in Fig. 2a, the TENG can be twisted 180° and crumpled without any breakage, which exposits a high softness. This feature indicates that the TENG can be well integrated into the fabric without being damaged by stretching or bending of the fabric. Fig. 2b and c demonstrated the tensile properties of the TENG with different conductive substrates, respectively. TENG with an aluminum foil as a conductive substrate broke at an elongation of about 25%, and the function of the generator is also lost. TENG with a fabric as a conductive substrate broken at an elongation of about 1300%. The elongation behavior below 400% is mainly the fracture of the fiber layer, which will not affect the function of generation. This also reflects the mechanical advantage of fabric as the conductive substrate. Compared with metal electrodes, traditional fabrics have excellent elastic properties and increase the service life of TENG. On the other hand, the air permeability of the aluminum foil is close to zero, and the air permeability of the conductive fabric is about 275 mm s^{-1} under constant pressure of 200 Pa, as shown in Fig. S7 in Supporting information. PCL acts as an adhesive to enhance the adhesion between the fiber membranes, as shown in Fig. 2d.

3.2. The electrical performance of TENG

To measure the output performance of the TENG (length, 80 mm; width, 40 mm) for mechanical energy harvesting and motion detection, a series of electrical signals were experimentally tested. Electrospun fiber membrane has the advantage of large specific surface area, which contributes large interfaces where PVDF and PA6 nanofibers lose and gain electrons during electrification. On the one hand, PANI has the characteristics of high conductivity. On the one hand, the conductive fabric and the friction material are well adhered by the PCL to improve the output performance. As revealed in Fig. 3a and b, the short-circuit current and open-circuit voltage output can arrive 200 μA and 1000 V, respectively.

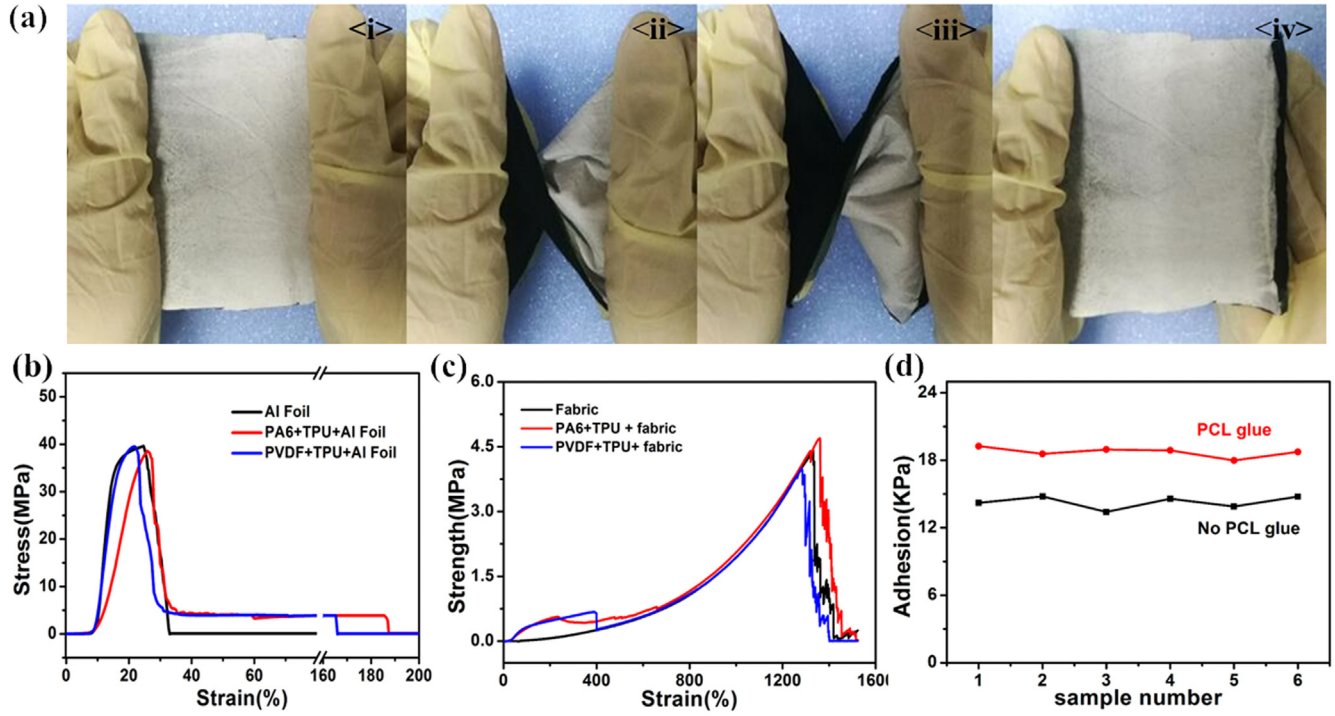

Fig. 2. (a) Flexibility of TENG. < i > Initial state, < ii > Twist 180° clockwise, < iii > Twist 180° counterclockwise, < iv > Restore. (b) Tensile properties measurement of the TENG that conductive substrate is aluminum foil. (c) Tensile properties measurement of the TENG that conductive substrate is fabric with in situ polymerization of PANI. (d) Fiber membrane adhesion test.

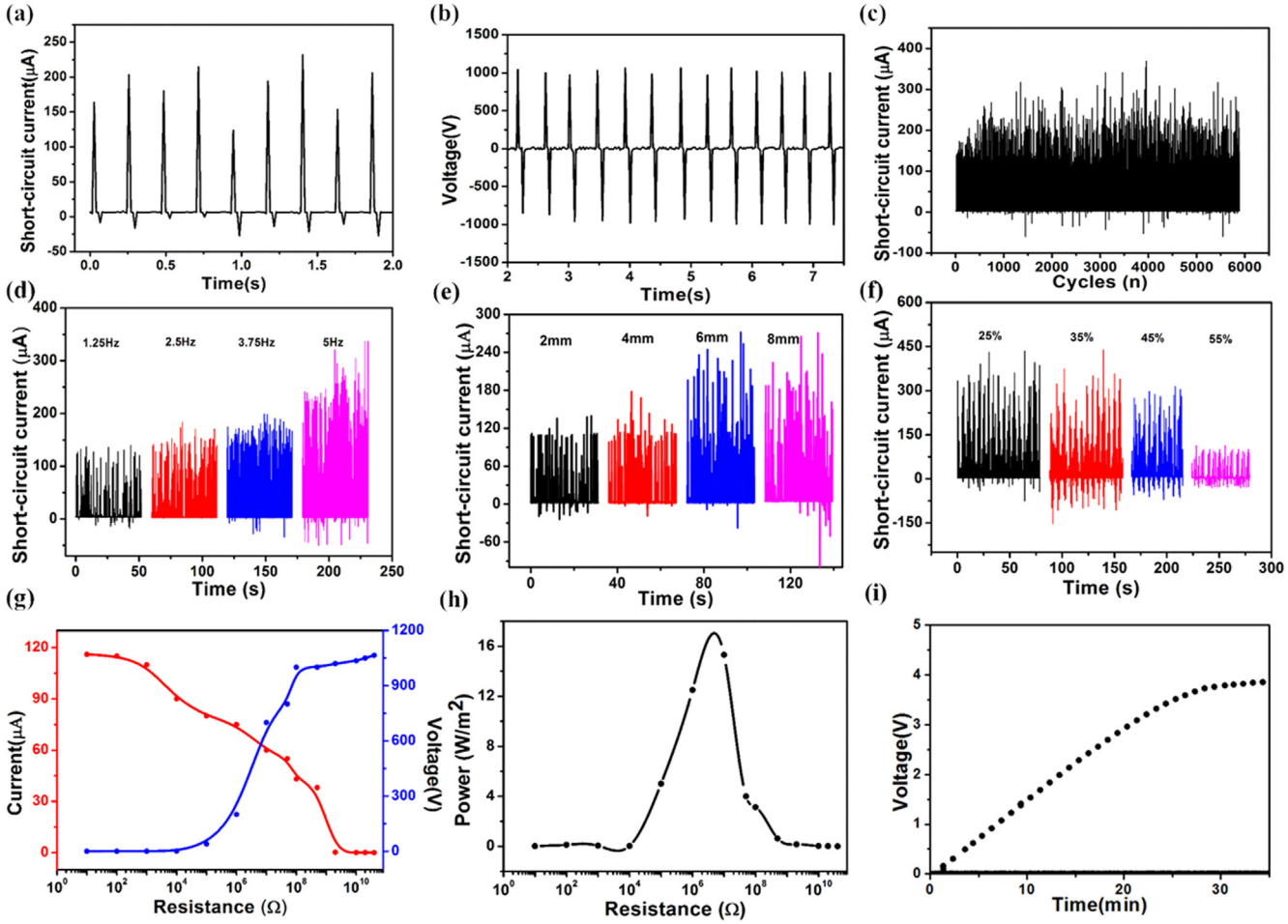

Fig. 3. Electrical performance of the TENG. (a) Short-circuit current and (b) open-circuit voltage of the TENG under the frequency of 2.5 Hz. (c) Electrical stability and durability test of the TENG. Short-circuit current of the TENG with different (d) impact frequency, (e) gap distance between the triboelectric materials and (f) atmospheric humidity. (g) Output current and voltage of TENG with various external load resistances. (h) Dependence of output power on load resistances. (i) Charging curve of a 47 μF commercial capacitor by the TENG.

The long-term stability/reliability of the TENG is essential concern in practical application. The output performance of the TENG is examined for over 5500 cycles at the same operation conditions. As demonstrated in Fig. 3c, the short-circuit current did not decrease, which represent an outstanding durability of the TENG.

To assess the adaptability of TENG to the environment, the output performance was tested under different impact frequency, gap distance between the triboelectric materials and atmospheric humidity. Fig. 3d shows with increasing impact frequencies, the short-circuit current of TENG increased proportionally. With the same charger gain/loss, higher impact frequency can shorten the sustained time of current peak, increasing the short-circuit current amplitude. Correspondingly, the open-circuit voltage showed the same trend with an increase of impact frequency in Fig. S4. As show in Fig. 3e, the short-circuit current increased and arrive a saturation trend gradually with an augment of distance between the triboelectric materials. Their open-circuit voltage is linearly proportional to the separation distance (Fig. S5) [43,44]. Environmental humidity can weaken the triboelectric effect and reduce the preservation time of triboelectric charges on the surfaces, according to Fig. 3f, as the atmospheric humidity decreases, the current increases.

The dependence of the electrical output signals on the load resistance has been systematically studied. As shown in Fig. 3g, the result shows that as the load resistance increases, the voltage tends to increase and the current shows opposite relation. We used the formula $P = \frac{U^2}{R}$ to get the power curve, the maximum load power density arrive 17.17 W m^{-2} with an external load resistance of 4.6 MΩ, as shown in Fig. 3h. The relative load voltage and current can reach 365 V and 65 μA respectively. TENG exhibits excellent output performance by comparison with other triboelectric nanogenerators, from the Table. S1 in Supporting information. The maximum power transfer occurs, if the external load is the same as the inherent impedance of the TENG [45,46], which made a certain theoretical basis for practical application.

Additionally, the pulse energy of TENG can be stored in a capacitor, Fig. 3i shows that a 47 μF commercial capacitor can be charged to 3.88 V at an operating frequency of 2.5 Hz, the gap distance of 6 mm, and a humidity of approximately 35%. The charging voltage can drive numerous small portable smart electronic devices, hence it has great development advantage in the field of portable self-generated devices.

As an energy generating device, TENG can supply efficient energy harvesting for multifarious applications. A TENG with the area of 10×10^2 1 cmwas adopt as an intuitive demonstration, Fig. 4a shows that a 47 μF commercial capacitor can be charged 4.5 V. From Fig. 4b and Video S1 in the Supplemental information, TENG could effectively illuminate approximately 1000 LEDs with high brightness. Therefore, we can combine LED and clothing as a self-powered warning garment for night-time workers to reduce the risk of danger. In addition, TENG can drive many electronic devices to work normally, as shown in Fig. 4c, d and e. The exemplary devices are electric watch, temperature-humidity sensor, and calculator. Demo operation (Video S2, S3 and S4) can be referred in the Supplemental information. Manifestly, smart fabric has an excellent capability of bio-energy collection and the applications of

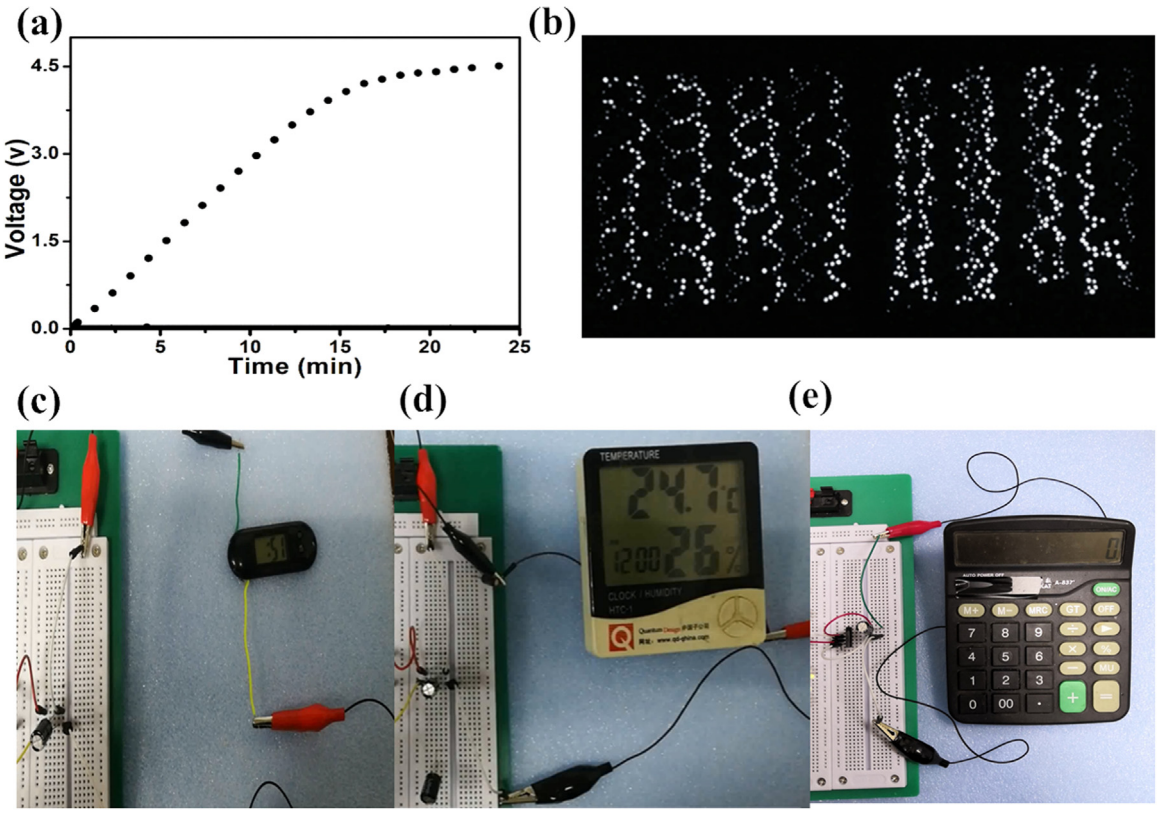

Fig. 4. Application of the 10x10 $cm^2$1 cmTENG in multiple devices. (a) Charging curve of 47 μF capacitor (b) Directly lighting up 944 LEDs without an extra storage power unit by a TENG working in human motion. Electronic devices driven by TENG, such as (c) electric watch, (d) temperature-humidity sensor, (e) and calculator.

TENG have a great potential in portable wearables, which are conducive to the popularity of NGs.

Supplementary material related to this article can be found online at doi:10.1016/j.nanoen.2019.01.069.

3.3. Application of TENG to harvesting energy and sensing

In addition to powering traditional equipment, a wearable TENG can be used in healthcare monitoring, as shown in Fig. 5a, application of wearable TENG to simulant hospital occasion for serious patient. As we all know that breathing is an important indicator for monitoring human vital signs and it represents the health of a person. If we wear clothes with respiratory monitoring, breathing sensor basing on masks can be replaced, which is helpful for the monitoring the breathing state continuously. TENG for human respiratory monitoring is shown in Fig. 5b. We collected output signals of the TENG in cases of normal breathing, deep breathing and rapid breathing (Fig. 5c). A threshold algorithm was used to determine long-term respiratory arrest. When the respiratory signal is below the threshold and the apnea time exceeds 10 s, the program will issue an early warning signal to illuminate the

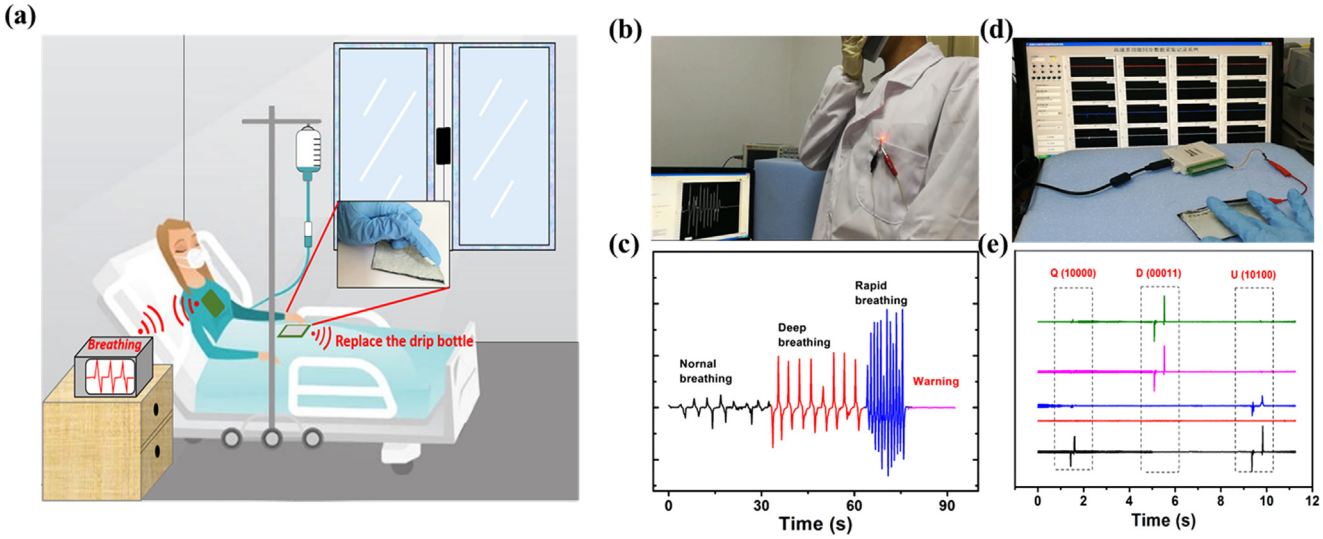

Fig. 5. (a) Wearable TENG for intensive care. (b and c) Photograph of respiratory monitoring and the corresponding output current. (d and e) Photograph of real-time communication based on fingers and corresponding output signals.

indicator light to predict the danger and avoid the tragedy, as demonstrate Video S5 in the Supplemental information. Such light can be replaced by other alarm systems to warn the guardian, which is applicable in situations of nursing critically ill patients or preventing child drowning events. As the Video S6 shows, in case of drowning, a warning signal will also be issued. Certainly it can also be worn on athletes to assess the athlete's physiological signals during exercise and performance indicators of body kinematics. During training, the athlete's breathing rate can be detected and collected in time using analog to digital conversion circuits and buffers. Without connecting any external equipment, such device will make the wearer move more naturally, with certain portability and comfort.

Supplementary material related to this article can be found online at doi:10.1016/j.nanoen.2019.01.069.

The health monitoring system can passively reflect the wearer's condition, and for special patients that wearing a breathing mask or unable to speak, using finger remote communication is also an important choice, such as the communication method used when Hawking's fingers are active , therefore, a real-time communicator was composed based on TENG. Put the positive triboelectric material was attached to fingers as shown in Fig. 5d. Thumb, index, middle, ring, and little fingers worked as five signal sources and they were numbered 1–5 respectively. The combinations of the output signals from each finger could compile all the alphabet. Detailed binary alphabet is shown in the support material (Table S2). As soon as gently touched, it will output an electrical signal and automated system could convert it into corresponding characters. As shown in Fig. 5e, output character “Q”, “D”, “U” were performed. Operation Video S7 can be referred in the Supplemental information. By wearing the fabric, real-time communication can be realized, and the electronic communication can be promoted in convenience.

Supplementary material related to this article can be found online at doi:10.1016/j.nanoen.2019.01.069.

In recent years, flexible electronic devices have received widespread attention. However, unlike the solder rigid connection of conventional electronic devices, the contact resistance is easily introduced during the use of flexible electronic devices. This results in an abnormal signal output from a resistive device, such as a piezoresistive device or a field effect device, which can seriously threaten the life of the patient being monitored. Fig. 6a demonstrates the change of the simulated respiratory signal through the voltage monitoring when the input current is constant after connecting an interference resistor. The threshold can be set reasonably before the access, so that the respiratory monitoring can be realized. However, after the interference resistor is connected, the threshold is lower than the overall signal. In this case, the alarm will never be set. The monitored signal is constantly larger than the threshold and no alarm will be set even in dangerous situation. Based on the possibility of such a false alarm state, the device needs to be calibrated to exclude contact resistance before each use, and the threshold value shall be modified according to such calibration. In stark contrast to this false alarm status, self-powered sensors do not need calibration before use. Fig. 6b shows the simulated respiratory signal of the self-powered sensor before and after the interference resistance is connected. Fig. S6 shows corresponding output current changes in Supporting information. It can be seen that the simulated respiratory signal does not change significantly before and after the resistance is connected, so the monitoring can be performed normally. Video S9 and S10 are placed in Supplementary materials as corresponding demonstration examples. This is due to the fact that the open circuit voltage will not be interfered by additional resistance in the circuit, which makes the self-powered sensor rather reliable when used in flexible circuit [47,48].

Supplementary material related to this article can be found online at doi:10.1016/j.nanoen.2019.01.069.

4. Conclusions

In summary, we reported a multifunctional wearable TENG. Ordinary fabric-polymerized PANI is used as electrodes. The electrodes are more flexible than conventional triboelectric structures, have gas permeability and are more suitable for wearable. We tested the electrical output of a TENG with an effective area of 4x8 cm^2 or 10x10 cm^2, the short-circuit current and open-circuit voltage output can arrive as high as 200 μA and 1000 V, respectively. The wearable TENG of 10×10 cm^2 can drive about 1000 LEDs. Its ability to continuously power electronic watch, temperature-humidity sensor, and calculator was also demonstrated. The TENG is rather helpful for the critically ill patients as a self-powered breath monitor and finger tapping communicator. The self-powered monitor was also proved to be more reliable than the resistive monitor when additional contact resistance was introduced, making it more applicable as flexible device. This advantage is of paramount importance for the research of self-powered sensors in the field of flexible devices.

Acknowledgements

This work was supported by the National Natural Science Foundation of China (51673103 and 11847135), the Shandong Provincial Natural Science Foundation, China (ZR2017BA013), the China Postdoctoral Science Foundation (2017M612200), and the

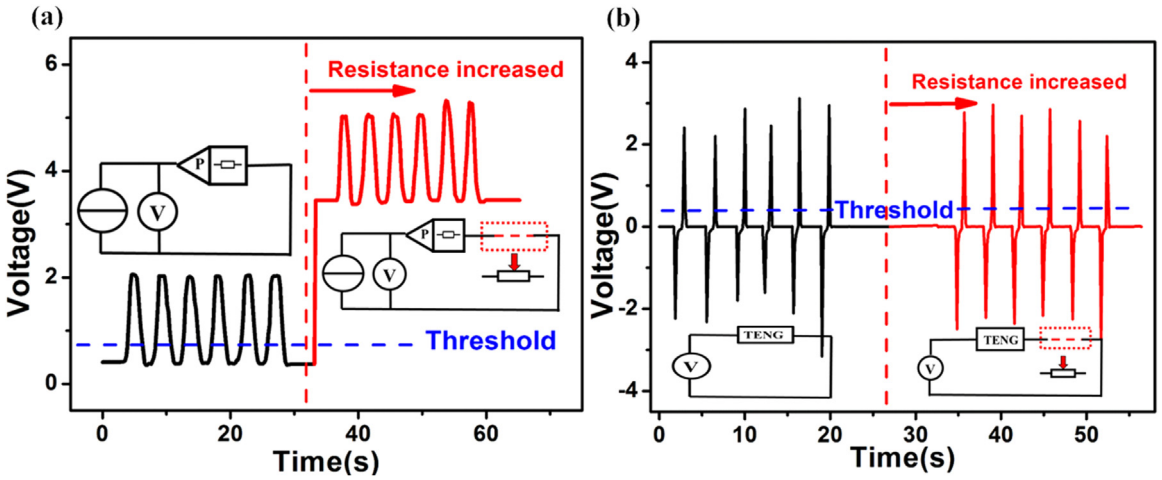

Fig. 6. (a) The changed output signal of the resistive sensor, due to poor contact of the line node, the loop resistance increases. (b) The output signal of the sensor based on TENG, due to poor contact of the line node, the loop resistance increases, but the output voltage remains unchanged.

Postdoctoral Scientific Research Foundation of Qingdao (2016007 and 2016014)

Appendix A. Supporting information

Supplementary data associated with this article can be found in the online version at doi:10.1016/j.nanoen.2019.01.069.

References

[1] Z.L. Wang, Mater. Today 20 (2017) 74–82.
[2] Z.L. Wang, J. Chen, L. Lin, Energy Environ. Sci. 8 (2015) 2250–2282.
[3] L. Serairi, L. Gu, Y. Qin, Y. Lu, P. Basset, Y. Leprincewang, Eur. Phys. J. Appl. Phys. 80 (2018) 30901.
[4] S.K. Karan, R. Bera, S. Paria, A.K. Das, S. Maiti, A. Maitra, B.B. Khatua, Adv. Energy Mater. 6 (2016) 1601016.
[5] S. Siddiqui, H.B. Lee, D.I. Kim, L.T. Duy, A. Hanif, N.E. Lee, Adv. Energy Mater. 8 (2018) 1701520.
[6] W. Wu, Nanotechnology 27 (2016) 112503.
[7] S.H. Baek, I.K. Park, Nanotechnology 28 (2017) 095401.
[8] X. Wang, W.Z. Song, M.H. You, J. Zhang, M. Yu, Z. Fan, S. Ramakrishna, Y.Z. Long, Acs Nano 12 (2018) 8588–8596.
[9] Y. Yang, Y. Zhou, J.M. Wu, Z.L. Wang, Acs Nano 6 (2012) 8456–8461.
[10] X. Wang, Y. Dai, R. Liu, X. He, S. Li, Z.L. Wang, Acs Nano 11 (2017) 8339–8345.
[11] F. Gao, W. Li, X. Wang, X. Fang, M. Ma, Nano Energy 22 (2016) 19–26.
[12] J. Qi, N. Ma, Y. Yang, Adv. Mater. 29 (2017) 1701189.
[13] M.H. You, X.X. Wang, X. Yan, J. Zhang, W.Z. Song, M. Yu, Z. Fan, S. Ramakrishna, Y.Z. Long, J. Mater. Chem. A 6 (2018) 3500–3509.
[14] Z. Quan, C.B. Han, T. Jiang, Z.L. Wang, Adv. Energy Mater. 6 (2016) 1501799.
[15] K. Dai, X. Wang, F. Yi, C. Jiang, R. Li, Z. You, Nano Energy 45 (2018) 84–93.
[16] R. Pan, W. Xuan, J. Chen, S. Dong, H. Jin, X. Wang, H. Li, J. Luo, Nano Energy 45 (2018) 193–202.
[17] W. Xu, L.B. Huang, M.C. Wong, L. Chen, G. Bai, J. Hao, Adv. Energy Mater. 7 (2016) 1601529.
[18] E.B. Araújo, E.C. Lima, I.K. Bdikin, A.L. Kholkin, J. Appl. Phys. 113 (2013) 146.
[19] F.R. Fan, W. Tang, Z.L. Wang, Adv. Mater. 28 (2016) 4283–4305.
[20] X.S. Zhang, M.D. Han, R.X. Wang, B. Meng, F.Y. Zhu, X.M. Sun, W. Hu, W. Wang, Z.H. Li, H.X. Zhang, Nano Energy 4 (2014) 123–131.
[21] F.R. Fan, Z.Q. Tian, Z.L. Wang, Nano Energy 1 (2012) 328–334.
[22] G. Zhu, Z.H. Lin, Q.S. Jing, P. Bai, C.F. Pan, Y. Yang, Y.S. Zhou, Z.L. Wang, Nano Lett. 13 (2013) 847–853.
[23] Q. Jing, G. Zhu, P. Bai, Y. Xie, J. Chen, R.P. Han, Z.L. Wang, Acs Nano 8 (2014) 3836–3842.
[24] P. Bai, G. Zhu, Y. Liu, J. Chen, Q.S. Jing, W.Q. Yang, J.S. Ma, G. Zhang, Z.L. Wang, Acs Nano 7 (2013) 6361–6366.
[25] G. Zhu, B. Peng, J. Chen, Q. Jing, Z.L. Wang, Nano Energy 14 (2015) 126–138.
[26] W. Jie, S. Li, Y. Fang, Y. Zi, J. Lin, X. Wang, Y. Xu, L.W. Zhong, Nat. Commun. 7 (2016) 12744.
[27] K.Y. Lee, J.S. Chun, J.H. Lee, K.N. Kim, N.R. Kang, J.Y. Kim, M.H. Kim, K.S. Shin, M.K. Gupta, J.M. Baik, S.W. Kim, Adv. Mater. 26 (2014) 5037–5042.
[28] F.R. Fan, W. Tang, Y. Yao, J. Luo, C. Zhang, Z.L. Wang, Nanotechnology 25 (2014) 135402.
[29] L. Zhang, F. Xue, W. Du, C. Han, C. Zhang, Z. Wang, Nano Res. 7 (2014) 1215–1223.
[30] T. Zhou, C. Zhang, C.B. Han, F.R. Fan, W. Tang, Z.L. Wang, Acs Appl. Mater. Interfaces 6 (2014) 14695–14701.
[31] W. Seung, M.K. Gupta, K.Y. Lee, K.S. Shin, J.H. Lee, T.Y. Kim, S. Kim, J. Lin, J.H. Kim, S.W. Kim, Acs Nano 9 (2015) 3501–3509.
[32] M. Zhang, T. Gao, J. Wang, J. Liao, Y. Qiu, Q. Yang, H. Xue, Z. Shi, Y. Zhao, Z. Xiong, Nano Energy 13 (2015) 298–305.
[33] H. Xue, Q. Yang, D. Wang, W. Luo, W. Wang, M. Lin, D. Liang, Q. Luo, Nano Energy 38 (2017) 147–154.
[34] Z. Li, J. Shen, I. Abdalla, J. Yu, B. Ding, Nano Energy 36 (2017) 341–348.
[35] W. He, H.V. Ngoc, Y.T. Qian, J.S. Hwang, Y.P. Yan, H. Choi, D.J. Kang, Appl. Surf. Sci. 392 (2017) 1055–1061.
[36] P. Vasandani, B. Gattu, J. Wu, Z.H. Mao, W. Jia, M. Sun, Adv. Mater. Technol. 2 (2017) 1700014.
[37] L. Tong, X.X. Wang, X.X. He, G.D. Nie, J. Zhang, B. Zhang, W.Z. Guo, Y.Z. Long, Nanoscale Res. Lett. 13 (2018) 86.
[38] R. Huang, Y.Z. Long, C.C. Tang, H.D. Zhang, Adv. Mater. Res. 853 (2013) 79–82.
[39] G.-F. Yu, X. Yan, M. Yu, M.-Y. Jia, W. Pan, X.-X. He, W.-P. Han, Z.-M. Zhang, L.-M. Yu, Y.-Z. Long, Nanoscale 8 (2016) 2944–2950.
[40] B.D. Chen, W. Tang, C. He, C.R. Deng, L.J. Yang, L.P. Zhu, J. Chen, J.J. Shao, L. Liu, Z.L. Wang, Mater. Today 21 (2018) 88–97.
[41] M. Willatzen, Z.L. Wang, Nano Energy 52 (2018) 517–523.
[42] Z.L. Wang, Acs Nano 7 (2013) 9533.
[43] S. Niu, Z.L. Wang, Nano Energy 14 (2015) 161–192.
[44] S. Niu, S. Wang, L. Lin, Y. Liu, Y.S. Zhou, Y. Hu, Z.L. Wang, Energy Environ. Sci. 6 (2013) 3576–3583.
[45] N. Kong, D.S. Ha, A. Erturk, D.J. Inman, J. Intell. Mater. Syst. Struct. 21 (2010) 1293–1302.
[46] M.N. Abdallah, T.K. Sarkar, M. Salazar-Palma, Maximum power transfer versus efficiency, in: Proceedings of the 2016 IEEE International Symposium on Antennas and Propagation, 2016, pp. 183–184.
[47] Y. Fang, X. Wang, S. Niu, S. Li, Y. Yin, K. Dai, G. Zhang, L. Lin, Z. Wen, H. Guo, Sci. Adv. 2 (2016) e1501624.
[48] F. Yi, J. Wang, X.F. Wang, S.M. Niu, S.M. Li, Q.L. Liao, Y.L. Xu, Z. You, Y. Zhang, Z.L. Wang, ACS Nano 10 (2016) 6519–6525.